NUMERICAL SIMULATION OF DESICCANT ASSISTED EVAPORATIVE COOLING SYSTEMS

Carlos Eduardo Leme Nóbrega, nobrega@pobox.com
Nísio Carvalho Lobo Brum, nisio@ufrj.com
Centro Federal de Educação Tecnológica Celso Suckow da Fonseca- CEFET-Rio. Av. Maracanã, 229 , DPMC, ZC.20271-110
Universidade Federal do Rio de Janeiro. PEM, COPPE, P.O. 68053, Rio de Janeiro, Brazil

Abstract. The use of evaporative cooling systems is traditionally limited to regions with very low average humidity levels, since it relies on the evaporation of water sprayed over an air stream to produce the cooling effect. Even under relatively dry conditions, the temperature drop on the fresh air stream is usually smaller when compared to vapor-compression cooling. Accordingly, the present work aims at comparing the performance of a evaporative cooling system with an without the assistance of a desiccant wheel. A mathematical model for the desiccant wheel is proposed and numerically solved using the finite volume technique, whereas the evaporative cooler performance is calculated by an effectiveness analysis. The use of evaporative cooling is usually restrained to climates with low average levels of relative humidity, nevertheless it was shown that the combination with solid desiccant systems has significantly widen the range of application of such systems. The results ratify the application of desiccant assisted evaporative cooling cycle as a promising technology to replace traditional vapor-compression cycles.

Keywords*: desiccant cooling, adsorption, evaporative cooling*

1. INTRODUCTION

One of the earliest efforts of modeling air dehumidification by a solid adsorbent was made by Trelkheld and Bullock (1966), which uses a predictor corrector method to obtain silica gel equilibrium data under adsorption conditions. Maclaine-Cross and Banks (1972) proposed a model in which the mass and energy equations were uncoupled under some simplifying assumptions. More recently, many numerical solutions have been provided, predominantly investigating the influence of thermal resistance to heat and different mass diffusion mechanisms within the desiccant material, such as Majundar (1998) and Zheng and Worek (1993). Zhang, Dai and Wang (2003) proposed a "lumped-distributed" model, which considered mass and temperature distributions only in the flow direction. The same approach was used by Spahier and Worek (2004), which performed a unified analysis for the heat and mass transfer mechanism. Camargo, Godoy and Ebinuma (2005) analyzed the influence of the regeneration temperature over the desiccant cooling cycle, using a simplified mathematical model based on prescribed effectiveness for each cycle component, whereas Nóbrega and Brum (2009) investigated the influence of different adsorptive materials over the desiccant cycle performance.

The use of evaporative coolers is however limited to areas with low average humidity levels, as it relies on the evaporation of water into the airstream to provide it with the cooling effect. Since the outlet temperature of the evaporative cooler is limited to the wet-bulb temperature of air inlet condition, such systems typically have to handle high airflow rates, so as to meet a given thermal load.

In any case, the lower the absolute humidity of the airstream, the higher will the cooling capacity evaporative unit. Therefore, if the air stream can be artificially dried before it is admitted to the evaporative unit, the achieved cooling effect would be much more significant.

Figure 1 shows the schematic representation of an evaporative cooling system, which can work with the assistance of a desiccant wheel (Figure 2). In the simple evaporative cycle, atmospheric air is fed directly to the evaporative cooler, where an adiabatic saturation process is carried out, lowering the airstream temperature with a corresponding increase in the absolute humidity. Accordingly, the airstream temperature drop strongly relies on the (low) absolute humidity of outside air.

In the desiccant assisted cycle, the fresh air stream is forced through a desiccant wheel, as it looses its humidity to the hygroscopic material. The exothermic nature of the adsorption processes, combined with the use of a thermal source to heat the exhaust stream and purge out the humidity, cause a temperature rise in the fresh air stream. Accordingly, the fresh air stream is cooled by successively forcing it through a regenerator and an evaporative cooler, where the cooling effect is achieved by spraying water over the low humidity fresh air stream. Therefore, the present work aims at comparing the lowest achievable temperatures by the evaporative cycle with and without the assistance of the desiccant wheel. Results show that the use of the desiccant unit can lower the outlet evaporator temperature as much as 5°C, when compared to the simple evaporative system, even for high relative humidity atmospheric conditions.

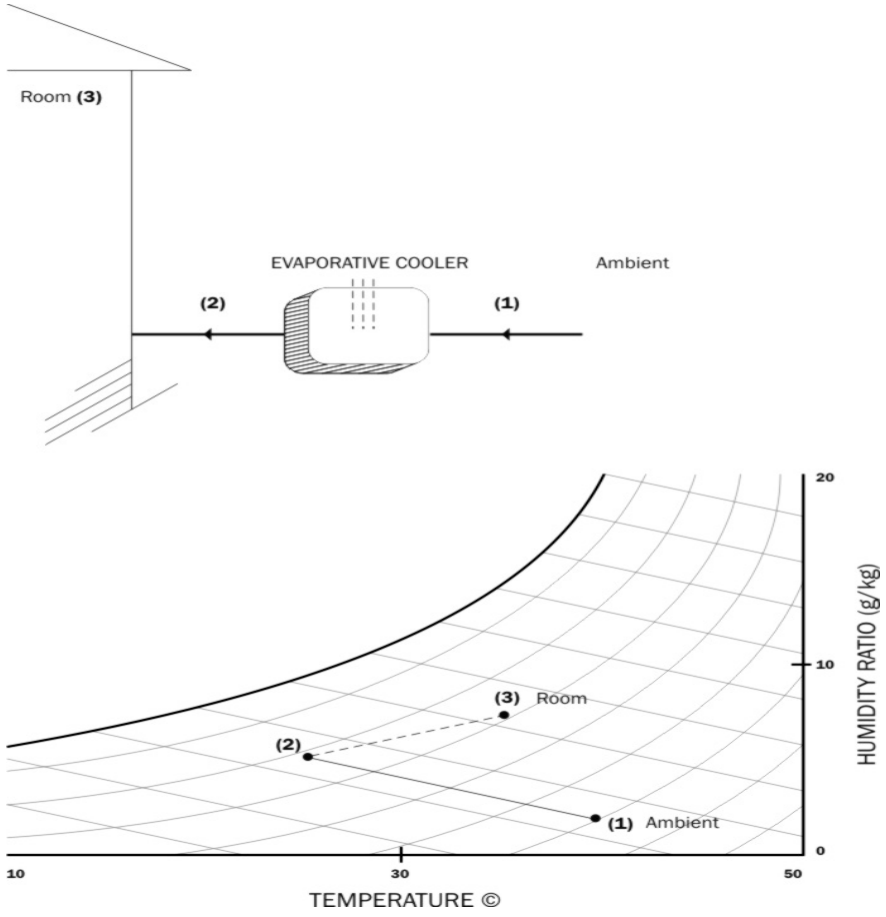

Figure 1: Schematic representation of a simple evaporative cooling cycle

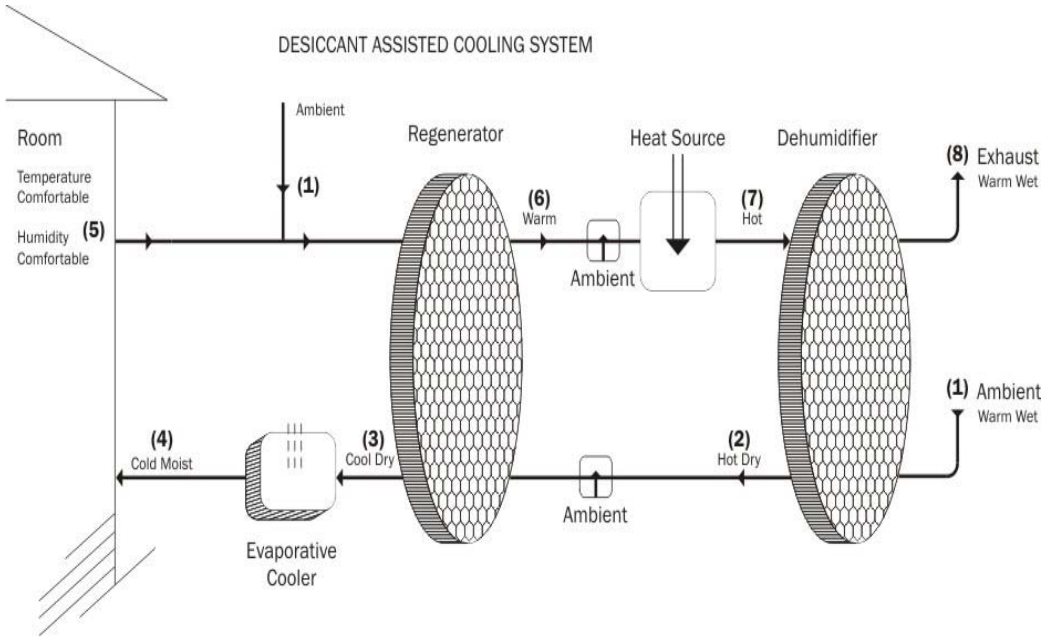

Figure 2: Schematic representation of a desiccant assisted evaporative cooling cycle

2. MATHEMATICAL MODELING

Consider a single channel detached from the wheel, as depicted in Figure 3. Air flows through the channel as it exchanges mass and heat with the hygroscopic walls.

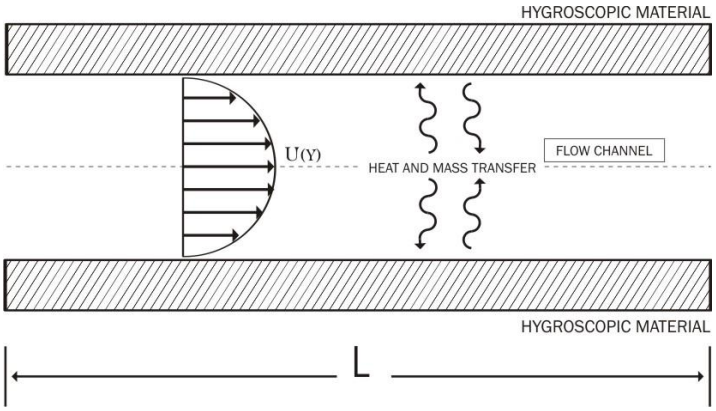

Figure 3: Schematic representation of a flow channel with desiccant walls

Some simplifying assumptions are required.

- The channels are perfectly insulated.
- All thermo-physical properties for the fluid and the solid are considered constant.
- The flow is hydro-dynamically and thermally developed.
- Temperature and concentration distributions in the direction normal to the flow are taken to be uniform (lumped) within the channel and the solid.
- The adsorption heat is modeled as a heat source within the solid material

Applying the mass conservation principle in a control volume enclosing the channel and the solid, as depicted in figure (4.a)

$$\dot{m}_1 \left[\frac{1}{u_1} \frac{\partial Y^*}{\partial t} + \frac{\partial Y^*}{\partial x} \right] + \frac{f\, m_w}{x_{AF}} \frac{\partial W}{\partial t} = 0 \qquad (1)$$

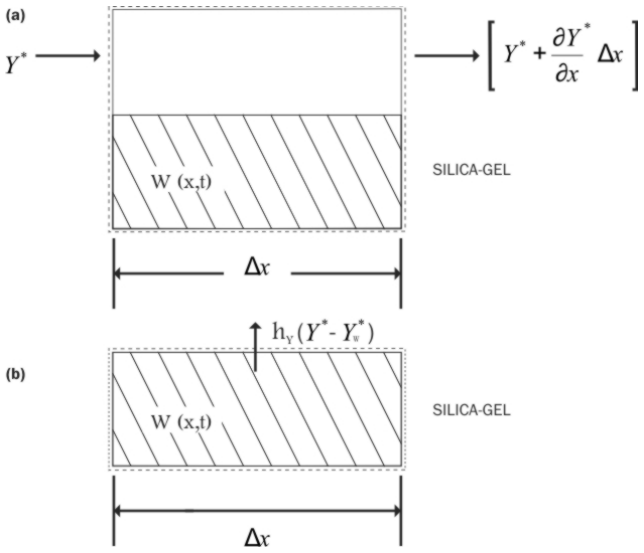

Figure 4: Mass balances within elementary control volumes

Applying the mass conservation principle in a control volume enclosing exclusively the solid, as depicted in figure (4.b),

$$\frac{f\ m_w}{x_{AF}\ y_{AF}}\frac{\partial W}{\partial t} = 2\,h_y\left(Y^* - Y_w^*\right) \tag{2}$$

Applying energy balance in a control volume enclosing the channel and the solid, as shown in Figure (5.a),

$$\dot{m}_1\left[\frac{1}{u_1}\frac{\partial H_1}{\partial t}+\frac{\partial H_1}{\partial x_A}\right]+\frac{m_w}{x_{AF}}\frac{\partial H_w}{\partial t} = 0 \tag{3}$$

Applying an energy balance in a control volume enclosing exclusively the channel, as shown in Figure (5.b),

$$\frac{\dot{m}_1}{y_{AF}}\left[\frac{1}{u_1}\frac{\partial H_1}{\partial t}+\frac{\partial H_1}{\partial x}\right] = 2\,h_y\left(Y_w^*-Y^*\right)\frac{\partial H_1}{\partial Y}+2\,h\left(T_w-T\right) \tag{4}$$

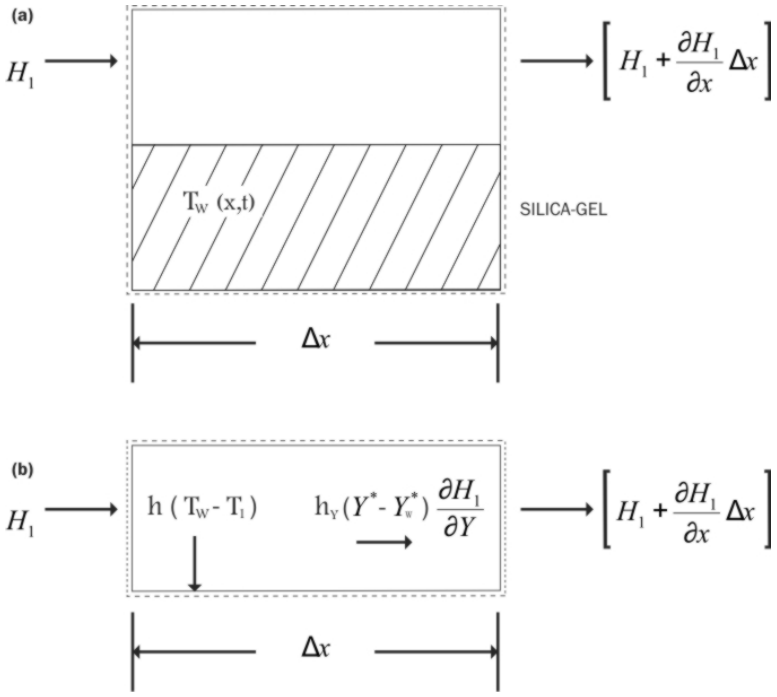

Figure 5: Energy balances within elementary control volumes

Defining the following parameters,

$$t_B = t-\frac{x}{u_1} \tag{5}$$

$$x^* = \frac{2h\,y_{AF}\,x}{\dot{m}\left(\frac{\partial H_1}{\partial T_1}\right)} \tag{6}$$

$$t^* = \frac{2\ h\ y_{AF}\ x\ t_B}{m_w C_w} \tag{7}$$

after extensive algebra, equations (1)-(4) can be written as

$$\frac{\partial Y^*}{\partial x^*} = Y_w^* - Y^* \tag{8}$$

$$\frac{\partial W}{\partial t^*} = \lambda_2 \left(Y^* - Y_w^* \right) \tag{9}$$

$$\frac{\partial T_1}{\partial x^*} = T_w - T_1 \tag{10}$$

$$\frac{\partial T_w}{\partial t^*} = \left(T_1 - T_w \right) + \lambda_1 \left(Y^* - Y_w^* \right) \tag{11}$$

in which

$$\lambda_2 = \frac{C_w}{f\left(\frac{\partial H_1}{\partial T_1} \right)} \tag{12}$$

$$\lambda_1 = \frac{\left(\frac{\partial H_1}{\partial Y} - \frac{1}{f}\frac{\partial H_w}{\partial W} \right)}{\left(\frac{\partial H_1}{\partial T_1} \right)} = \frac{Q}{\left(\frac{\partial H_1}{\partial T_1} \right)} \tag{13}$$

$$Q = \frac{\partial H_1}{\partial Y} - \frac{1}{f}\frac{\partial H_w}{\partial w} \tag{14}$$

where Q represents the heat of sorption, as suggested by Zhang, Dai and Wang (2003)

$$Q = h_v \left(1.0 + 0.284 e^{-10.28W} \right)$$

The parameter C_w in Eq.(12) represents the specific heat of the wall, which is highly dependent of its humidity content W,

$$H_w = T_w f\, W\, C\ + f\, \Delta H_w \tag{15}$$

$$\frac{\partial H_w}{\partial T_w} = C_w = f\, W\, C + f\, \frac{\partial \Delta H_w}{\partial T_w} \tag{16}$$

and this causes Eq. (9) to be non-linear. Close and Banks (1972) showed the last term of the right-hand side of Eq. (15) contributes with less then 2% of the value of C_w, and thus can be neglected. Now its necessary to evaluate the derivatives of the air enthalpy H_1, as required by Eqs. (12) and (13). The specific enthalpy of the air H_1 can be written as

$$H_1 = aT_1 + Y^* \left(d + cT_1 \right) \tag{17}$$

with its derivative with respect to the temperature is given by

$$\frac{\partial H_1}{\partial T_1} = a + cY \tag{18}$$

and its derivative with respect to the absolute humidity is given by

$$\frac{\partial H_1}{\partial Y} = d + cT_1 \tag{19}$$

where

$$a = 1.00 KJ / Kg\ ^{\circ}C$$
$$d = 2501 KJ / Kg$$
$$c = 1.86 KJ / Kg\ ^{\circ}C$$

The adsorption isotherm for silica-gel (Pesaran and Mills, 1987) relates the relative humidity of the air layer to the wall temperature (T_w) and humidity content (W),

$$\phi_w = 0.078 - 0.0579W + 24.16554W^2 - 124.78W^3 + 204.226W^4 \tag{20}$$

the Antonine equation gives the pressure of saturated water vapor,

$$P_{ws} = \mathrm{e}^{\left(23.196 - \frac{3816.44}{T_w - 46.13}\right)} \tag{21}$$

and the relationship between humidity and relative humidity is given by Eq.(22).

$$Y_w = \frac{0.62188 P_w}{P_{atm} - P_w} = \frac{0.62188 \phi_w}{\frac{P_{atm}}{P_{ws}} - \phi_w} \tag{22}$$

There is a set of four partial differential equations to be solved (8-11), along with one algebraic equation (Eq.22). Accordingly, there are five unknowns, T_1, T_w, W, Y_1 and Y_w. Equations (14) to (19) define auxiliary parameters to evaluate equations (12) and (13), whereas equations (20) and (21) are auxiliary equations to evaluate Eq. (22). One should note that the heat of sorption Q also depends on the wall humidity content W, which couples the heat and mass transfer problems. Moreover, the periodic nature of the problem requires an iterative procedure, since both initial distributions of temperature and humidity within the extension of the wheel are not known beforehand. Boundary conditions are given by

$$T_1(0, t^*) = T_{hi} \qquad , 0 < t^* < P_h^* \tag{23}$$

$$Y_1(0, t^*) = Y_{hi} \qquad , 0 < t^* < P_h^* \tag{24}$$

$$T_1(x_f^*, t^*) = T_{ci} \qquad , P_h^* < t^* < P^* \tag{25}$$

$$Y_1(x_f^*, t^*) = Y_{ci} \qquad , P_h^* < t^* < P^* \tag{26}$$

and the periodicity conditions are given by

$$T_{wc}(x^*, P^*) = T_{wh}(x^*, 0) \tag{27}$$

$$W_c(x^*, P^*) = W_h(x^*, 0) \tag{28}$$

3. Numerical Solution

Equations (8) and (10) are integrated in space, whereas equations (9) and (11) are integrated in time, both using the finite volume method (Patankar, 1980). The temperature and humidity at the boundaries of the elements of the convective equations (8) and (10) are represented by the upwind scheme; whereas the transient terms present in equations (9) and (11) are represented by a fully-implicit formulation. The periodic nature of the problems requires an iterative solution, since the initial distributions of temperature and humidity are unknown. Accordingly, the temperature field T_w and the humidity field W within the solid material are initially guessed, and the tridiagonal systems obtained by the discretization of Eqs. (8) - (11) are solved for successive time steps until the non-dimensional period of revolution P^* is reached. For steady-state operation, the temperature and humidity fields calculated at the end of non-dimensional period ($t^* = P^*$) must exactly match the fields at the beginning ($t^* = 0$), T_w (guess) and W(guess). The process is repeated using the calculated fields as new guesses for the initial distributions, until both humidity and temperature criteria have been attained, and the solution has converged. Since the control-volume regime is periodic, the inlet of enthalpy must equal the average outlet enthalpy, as required by the heat and mass balance error,

$$Crit.\ \ Conv._{temp} = \frac{T_w(x^*,P^*) - T_w(guess)(x^*,0)}{T_w(x^*,P^*)} \tag{29}$$

$$Crit.\ \ Conv._{mass} = \frac{W(x^*,P^*) - W(guess)(x^*,0)}{W(x^*,P^*)} \tag{30}$$

$$HMBE = \frac{\dot{m}_h H_{1hi} + \dot{m}_c H_{1ci} - (\dot{m}_h \frac{1}{p_h}\int_0^{p_h} H_{1ho}\, dt^* + \dot{m}_c \frac{1}{p_c}\int_0^{p_c} H_{1co}\, dt^*)}{\dot{m}_h H_{1hi} + \dot{m}_c H_{1ci}} \tag{31}$$

4. RESULTS

Figures 4 and 5 show a comparison between the simple and desiccant assisted evaporative cooling systems, for a moderate and a high ambient temperature values. It can be seen that even for high values of relative humidity, the use of a desiccant wheel enables a significant lower temperature at the outlet of the evaporative cooler device. This effect is more pronounced at moderate values of the ambient temperature (Fig. 5), which can be explained by the progressive loss of adsorptive capacity exhibited by the silica-gel (a general behavior exhibited by many other solid adsorbents) with increasing temperature. Figure 5 shows that the difference between the outside and room temperature can be as high as 8ºC - even for a high relative humidity of 80% - which evidences the use of a desiccant assisted evaporative cooling a promising technology. Figures 6 and 7 show the effect of increasing the regeneration temperature over the evaporative cooler outlet temperature, for two different levels of ambient temperature. In all cases, an increase in the regeneration temperature will allow a decrease in the evaporative cooler outlet temperature, which can be justified by the cyclic nature of the dehumidifying process. The higher the regeneration temperature, the lesser will be the humidity content within the solid by the end of the desorption period, consequently allowing a greater available volume of dry desiccant material for the adsorption period. Overheating of the process air stream is not of concern, since it will be regenerated after it leaves the desiccant wheel, as depicted in Fig 2.. Therefore, an increased dehumidifying capacity will be achieved by a higher regeneration temperature, allowing lower temperatures at the evaporative cooler outlet. This result contradicts the results found by Camargo, Godoy and Ebinuma (2005).

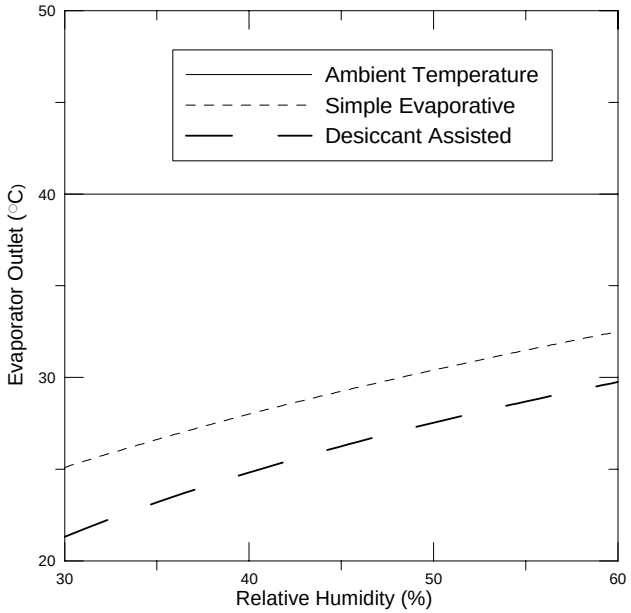

Figure 4. Evaporator outlet temperature for a high ambient temperature (40°C)

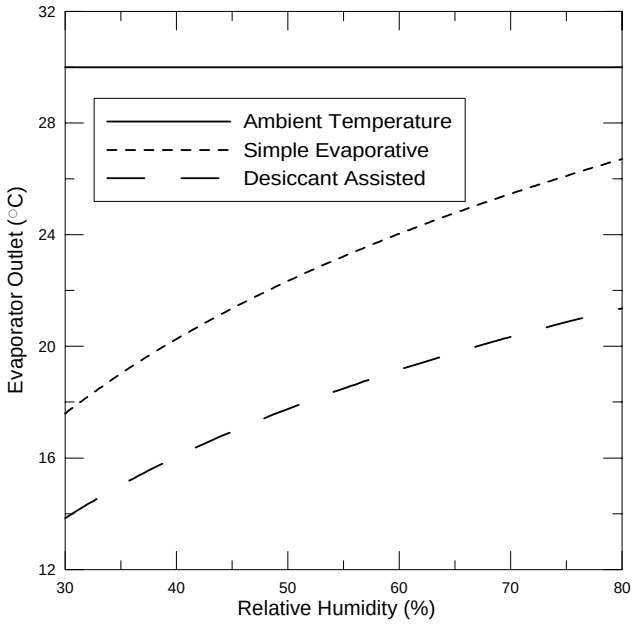

Figure 5. Evaporator outlet temperature for a moderate ambient temperature (30°C)

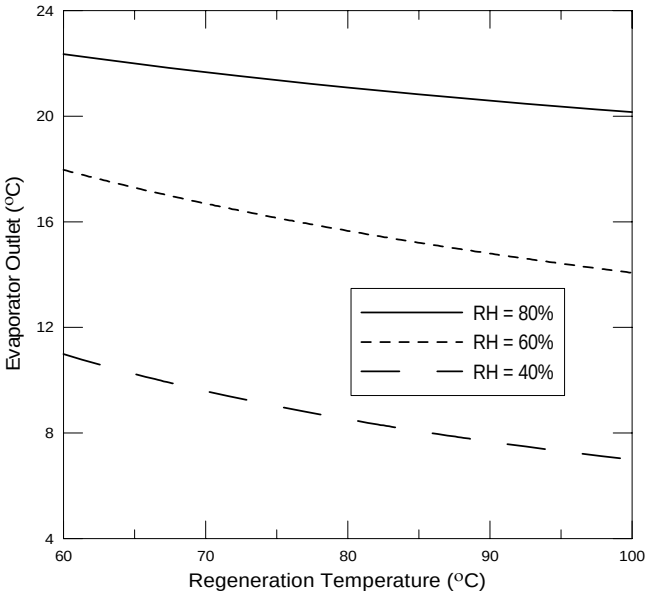

Figure 6. Evaporator outlet temperature as a function of regeneration temperature, T_{ci} = 30ºC

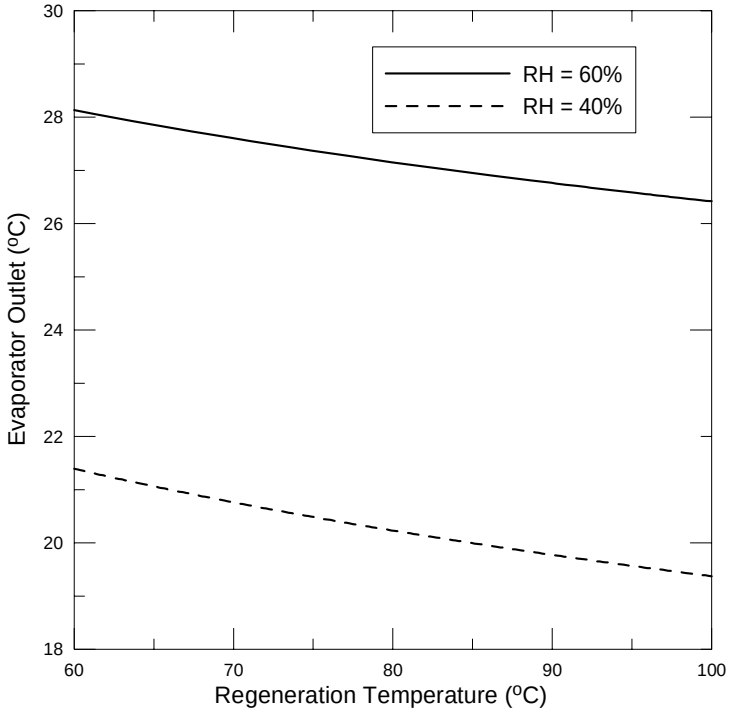

Figure 7. Evaporator outlet temperature as a function of regeneration temperature, T_{ci} = 40ºC

5. CONCLUSION

A mathematical model for a solid adsorbent heat and mass transfer exchanger was developed under some simplifying assumptions. The resulting set of four partial differentials and one algebraic equation was numerically solved by a discretization technique, allowing the dynamic behavior of the desiccant wheel to be predicted. It was shown that the evaporative cooler outlet temperature can be significantly decreased with the use of a desiccant wheel, allowing an appreciable cooling effect even in a climate with high average moisture levels. It was also shown that the evaporative cooler outlet temperature slightly decreases with the increase of the regeneration temperature, which is consonant to the improved dehumidifying capacity allowed by a higher temperature. This effect has been reported to be more significant in stronger adsorbents such as molecular sieve 13A (Nóbrega and Brum (2009)).

NOMENCLATURE

C	specific Heat of the desiccant material
C_w	specific Heat of the wall
f	desiccant mass fraction
h	heat transfer coefficient (kW/m^2)
H	enthalpy of air (kJ/kg)
h_y	convective mass transfer coefficient (kg/m^{2}s)
h_v	heat of Vaporization (kJ/kg)
$\dot{m}$	air mass flow rate (kg/s)
m_w	mass of the wall (kg)
P	period of revolution (s)
P_{atm}	atmospheric Pressure (Pa)
P_{ws}	saturation Pressure (Pa)
Q	heat of adsorption (kJ/kg)
t	time (s)
T	temperature (°C)
u	in flow velocity (m/s)
W	desiccant humidity (kg of moisture/kg of desiccant)
x	coordinate (m)
X_{AF}	length of the wheel (m)
Y	absolute Humidity (kg/kg air)
y_{AF}	flow channel width (m)

Greek letters

λ_1 auxiliary parameter

λ_2 auxiliary parameter
ϕ_w humidity of air layer
ε effectiveness

Subscripts

f channel length
w wall
wc wall during cold period
wh wall during hot period
hi hot inlet
ho hot outlet
ci cold inlet
co cold outlet
h hot period
c cold period
1 air

5. REFERENCES

Bullock, C.E.; Threlkheld, J.L. 1966, "Dehumidification of Moist Air by Adiabatic Adsorption", Transactions of ASHRAE, 72 (1), pp.301-313.

Banks, P.J., Close, .J. 1972, "Coupled Heat and Mass Transfer in Regenerators", International Journal of Heat and Mass Transfer, vol. (15), pp.1225-1242.

Camargo, J.R., Godoy, E., Ebinuma, C.D., 2005, "An Evaporative and Desiccant Cooling System for Air Conditioning in Humid Climates", J. Braz. Soc. Mech. Sci. & Eng., vol. (27), no.3, pp.1-11.

Kays, W.M.; London, A.L., "Compact Heat Exchangers", 3rd ed., McGraw-Hill, New York, 1984.

Maclaine-Cross, I.L.; Banks, P.J., 1972, "Coupled Equilibrium Heat and Single Adsorbate Transfer in Fluid Flow through Porous Media", International Journal of Heat and Mass Transfer, vol. (27), pp. 1157-1169.

Majumdar, P., 1998, "Heat and Mass Transfer in Composite Desiccant Pore Structures for Dehumidification", *Solar Energy*, vol. (62), pp.1-10.

Nóbrega, C.E.L., Brum, N.C.L., 2009, "Influence of Isotherm Shape over Desiccant Cooling Cycle Performance", Heat Transfer Engineering, vol.30 (4), pp.322-328.

Patankar, S. "Numerical Heat Transfer and Fluid Flow", Hemisphere Publishing Co., Boston, 1980.

Pesaran, A.A., Mills, A.F..; 1987, "Moisture Transport in silica Gel Packed Beds-Part I", International Journal of Heat and Mass Transfer, vol.30, pp. 1051-1060.

Sphaier, L.A.; Worek, W.M., 2004, "Analysis of Heat and Mass Transfer in Porous Adsorbents Used in Rotary Regenerators", International Journal of Heat and Mass Transfer, vol. 47, pp.3415-3430.

Zheng, W.; Worek, W.M., 1993; "Numerical Simulation of Heat and Mass Transfer Processes in a Rotary Dehumidifier", Numerical Heat Transfer, A, vol.23, pp.211-232.

Zhang, X.J., Dai, Y.J., Wang, R.Z.; 2003, "A Simulation Study of Heat and Mass Transfer in a Honeycomb Structure Rotary Desiccant Dehumidifier", Applied Thermal Engineering (23), pp 989-1003.

.

5. RESPONSIBILITY NOTICE

The authors are the only responsible for the printed material included in this paper.